

PAPER

Energy efficient hopping with Hill-type muscle properties on segmented legs

To cite this article: Andre Rosendo and Fumiya Iida 2016 *Bioinspir. Biomim.* **11** 036002

View the [article online](#) for updates and enhancements.

Related content

- [The role of intrinsic muscle properties for stable hopping](#)
D F B Haeufle, S Grimmer and A Seyfarth
- [Stretch reflex improves rolling stability during hopping of a decerebrate biped system](#)
Andre Rosendo, Xiangxiao Liu, Masahiro Shimizu et al.
- [Stance leg control](#)
Sebastian Riese and Andre Seyfarth

Recent citations

- [Biarticular elements as a contributor to energy efficiency: biomechanical review and application in bio-inspired robotics](#)
Karen Junius et al



IOP | ebooks™

Bringing you innovative digital publishing with leading voices to create your essential collection of books in STEM research.

Start exploring the collection - download the first chapter of every title for free.

Bioinspiration & Biomimetics



PAPER

Energy efficient hopping with Hill-type muscle properties on segmented legs

Andre Rosendo and Fumiya Iida

Department of Engineering, The University of Cambridge, Cambridge, UK

E-mail: andre.rosendo@eng.cam.ac.uk

Keywords: energy efficiency, hopping, Hill-type muscle, CoH, intrinsic muscle properties

RECEIVED
7 October 2015

REVISED
22 March 2016

ACCEPTED FOR PUBLICATION
23 March 2016

PUBLISHED
12 April 2016

Abstract

The intrinsic muscular properties of biological muscles are the main source of stabilization during locomotion, and superior biological performance is obtained with low energy costs. Man-made actuators struggle to reach the same energy efficiency seen in biological muscles. Here, we compare muscle properties within a one-dimensional and a two-segmented hopping leg. Different force–length–velocity relations (constant, linear, and Hill) were adopted for these two proposed models, and the stable maximum hopping heights from both cases were used to estimate the cost of hopping. We then performed a fine-grained analysis during landing and takeoff of the best performing cases, and concluded that the force–velocity Hill-type model is, at maximum hopping height, the most efficient for both linear and segmented models. While hopping at the same height the force–velocity Hill-type relation outperformed the linear relation as well. Finally, knee angles between 60° and 90° presented a lower energy expenditure than other morphologies for both Hill-type and constant relations during maximum hopping height. This work compares different muscular properties in terms of energy efficiency within different geometries, and these results can be applied to decrease energy costs of current actuators and robots during locomotion.

1. Introduction

Animals move in a plethora of gaits with different energy consumptions. Among these gaits, the hopping gait is the first choice of many animals, and can also be considered as a widely accepted simplification of the running gait [1]. The importance of understanding how leg and body behave during hopping has prompted scientists to conduct biological experiments focusing on this gait. One-legged hopping experiments with humans pointed to the existence of a preferred hopping frequency which maximizes the effects of the stretch reflex [2], while other experiments with hopping and jumping subjects suggested that the suppression of the *H*-reflex changes the behavior of human muscles from springs to dampers [3].

Whenever biological experiments are limited by biological factors, simulations can, to some extent, explain locomotory phenomena and provide new insights on how animals move. Hopping simulations considering a two-segmented leg with a positive force feedback suggested that this proposed stretch reflex

can stabilize running behavior and act as a replacement for central motor commands [4]. From a biomimetic perspective [5], experiments with artificial muscles within a musculoskeletal biped proved that the presence of stretch reflex helps stabilization on the frontal plane [6]. The integration of such feedback properties with feed-forward control within different muscle architectures can be seen in [7]. There, force–length and force–velocity relations are simulated with a one-dimensional linear hopping muscle as constant, linearly increasing, or Hill-type behavior, and they proved that the Hill-type muscle recovered from disturbances faster than other architectures. A similar work from the same author [8] focused on the intrinsic properties of muscles with the same one-dimensional hopping muscle, and the author concluded that force–length relation has a very low contribution to stability, while linear and Hill-type force–velocity relations increased stability.

Beyond locomotory stability, energy expenditure is another remarkable feature observed in animals, which allows longer periods without food and thus a

higher chance of survival. The manifold implications of a lower energy consumption is such that it can also be used to trace the human transition from quadrupedal to bipedal locomotion [9]. While energy efficiency has been studied from a biological perspective [10], only a few works recreate locomotion to understand how energy is used. From passive walkers [11] to regenerating electric quadrupeds [12], roboticists aim to reduce energy consumption to increase autonomy, with special attention to the works of [13, 14]. While the former presents a beam hopper which explores the natural frequency of the system to perform vertical hops, the latter adopts a parallel elastic actuator with an open-loop sinusoidal control to horizontally displace the hopping robot. Nonetheless, studies regarding the energy efficiency of muscular properties during locomotion are, to the best of the author's knowledge, nonexistent.

In this work we propose a vertical hopping simulation to better understand the influence of muscular properties on energy efficiency. We adopted two hopping models—a one-dimensional linear model and a two-segmented leg model—and used three different simplifications for the force–length and force–velocity behaviors—constant, linear, and Hill-type. With a total of nine cases per model, we simulate stable hops with the proposed 18 cases, and estimate the cost of hopping (CoH) for each one of them. Additionally, we compare their CoH while hopping at the same height. Beyond previous works in the area [8], we aim to show that the introduction of nonlinearity on locomotion, inherent to segmented limbs, alters the hopping behavior of the model. We also aim to understand the impact of force–length and force–velocity relations on the energy expenditure, going beyond an understanding of hopping stability. Our conclusions suggest that biological muscles and geometries are optimized for efficiency, and better actuators should follow similar cues to improve autonomy in robots.

In section 2, we introduce the hopping models and the parameters adopted during simulation. In section 3, we present the results from our hopping experiments, and in section 4, we discuss these results and conclude this paper.

2. Methods

Hopping can be considered as a horizontal [14, 15] or a vertical [16] motion, and within this work we will focus on the vertical aspects of this movement. While simplifying this vertical motion as a mass attached to one leg might deprive our studies from intricate details from the motion observed in animals, this simplification guides us to the essence of the movement, which leaves the aforementioned details to be subject of different studies.

Our simulations adopted two different models: the first, known as the linear model, is a one-dimensional

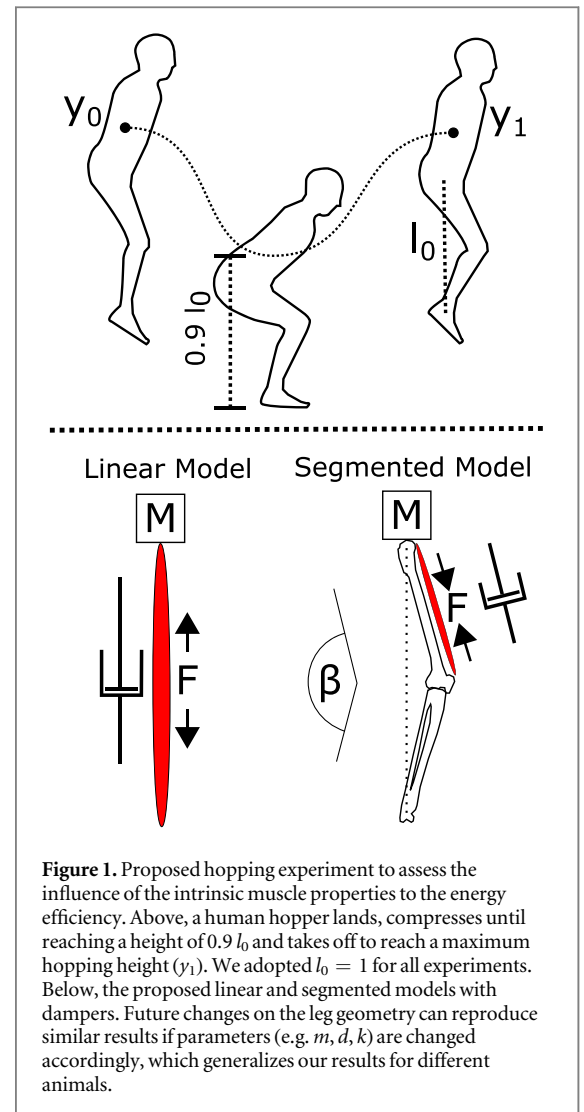
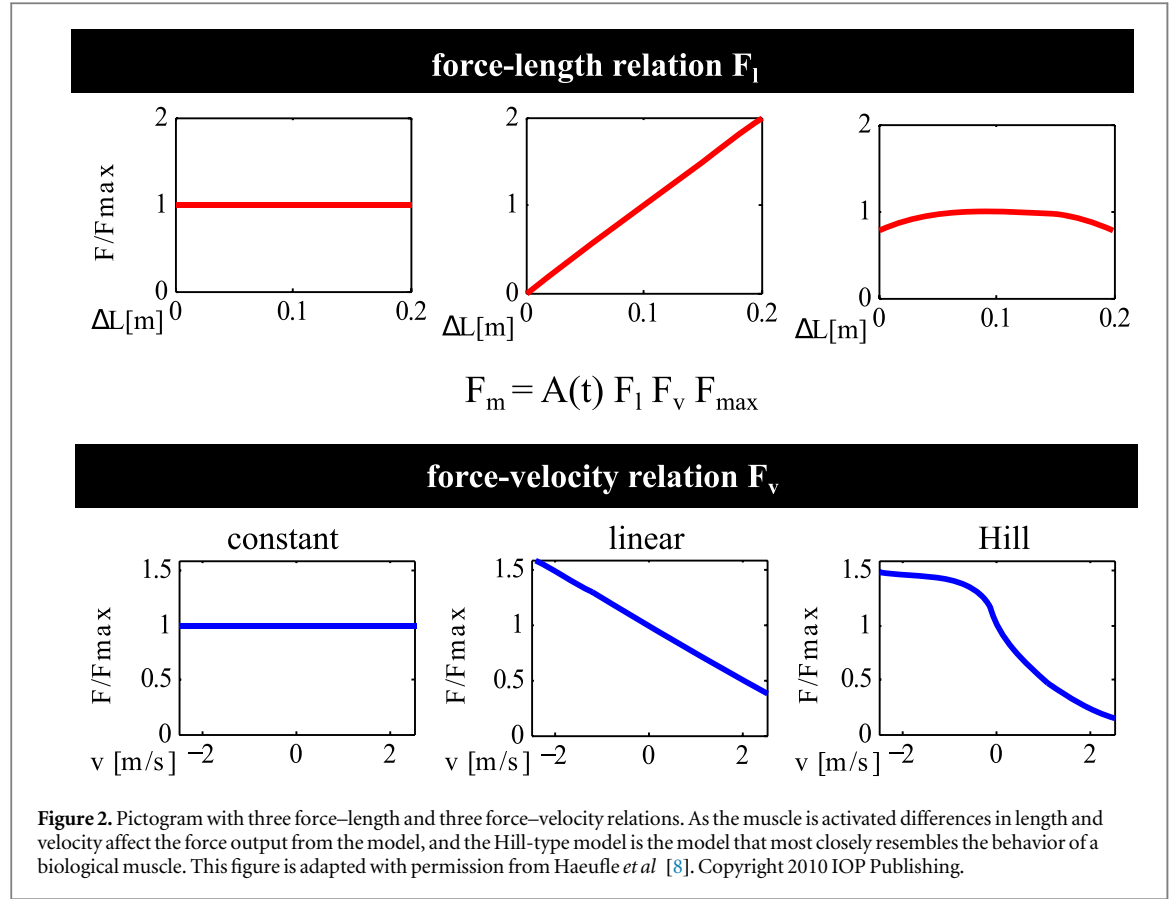


Figure 1. Proposed hopping experiment to assess the influence of the intrinsic muscle properties to the energy efficiency. Above, a human hopper lands, compresses until reaching a height of $0.9 l_0$ and takes off to reach a maximum hopping height (y_1). We adopted $l_0 = 1$ for all experiments. Below, the proposed linear and segmented models with dampers. Future changes on the leg geometry can reproduce similar results if parameters (e.g. m, d, k) are changed accordingly, which generalizes our results for different animals.

muscle which expands when actuated, and the second model, known as segmented model, is a two segmented leg with a monoarticular knee-extending muscle, similar to a vastus lateralis. The reason for adopting two models instead of one is to compare the behavior of a linear and a nonlinear morphology to the influence of different muscle properties. In stark difference from previous works [4, 8], we compare the influence of these two morphologies to the energy efficiency of the system and systematically change the resting angle to understand the observed differences. In figure 1 both models are compared to a hopping human, and a damping element was introduced to force the muscle to reconstitute the energy losses. We measure energy efficiency by accounting the energy spent in this corrective measure.

2.1. Linear model

As shown in figure 1, we idealized the leg as a single expanding massless muscle with the body mass on top of it. The model falls from a predefined height y_0 , touches the floor, compresses the muscle until it reaches the mid-stance with a leg compression of



0.1 m, and propels itself upwards to reach the final height of y_1 . Our simulations considered the hopping as a hybrid dynamic system, with a flight and a stance phase, and the equation of motion is defined as

$$m\ddot{y} = -mg + \begin{cases} 0 & \text{if } y > l_0 \\ F_m + d\dot{y} & \text{otherwise,} \end{cases} \quad (1)$$

where m is the total mass of the system, y is the vertical position of the center of mass, d is the damping coefficient during stance, l_0 is the rest length of the muscle, and F_m is the total force applied by the muscle against the floor. F_m is a combination of the activation, force–length–velocity relations and maximum force, and is described by the following equation:

$$F_m = A(t) F_l F_v F_{\max}. \quad (2)$$

This model is, for the sake of comparison, largely based on a similar model presented in [8] with the addition of damping losses. The force–length and force–velocity relations also follow similar comparison, expressed by

$$F_l = \begin{cases} 1 & \text{Constant} \\ k(l_0 - l) & \text{Linear} \\ \exp\left[c \left| \frac{l - l_{\text{opt}}}{l_{\text{opt}} w} \right|^3\right] & \text{Hill, and} \end{cases} \quad (3)$$

$$F_v = \begin{cases} 1 & \text{Constant} \\ 1 - \mu v & \text{Linear} \\ \frac{v_{\max} + v}{v_{\max} - Kv} & \text{Hill } (v > 0) \\ N + (N - 1) \frac{v_{\max} - v}{-7.56Kv - v_{\max}} & \text{Hill } (v \leq 0), \end{cases} \quad (4)$$

where k is the spring coefficient for the linear behavior, l is the leg length, c is the curvature of the bell-shaped force–length relation approximation for Hill-type behavior, w is the width of this curvature, and l_{opt} is the optimal length for maximum force output. Within the force–velocity relation μ is the angular coefficient of the linear behavior, v_{\max} is the maximum velocity output, K is the curvature constant, N is the dimensionless force F_m/F_{\max} at maximum velocity. Figure 2 depicts the force–length and force–velocity behaviors during muscular activation.

The parameters for this experiment are shown in table 1, and the rationale for these choices is to mimic observations with human experiments and simulations [4]. Similar observations from the same work will also be the basis for the idealization of the segmented model.

2.2. Segmented model

As with the linear model, the segmented model consists of a body mass attached to the upper part of a massless leg. The main difference between these models lies in the presence of a joint and two links,

Table 1. Hopping model parameters.

| Parameter | Linear model | Segmented model |
|---|------------------------|-----------------------|
| Leg rest length l_0 | 1 m | 1 m |
| Body mass m | 80 kg | 80 kg |
| Gravitational constant g | 10 m s ⁻² | 10 m s ⁻² |
| Maximum muscle force F_{\max} | 2.5 kN | 19.8 kN |
| Spring coefficient for linear behavior k | 10 m ⁻¹ | 100 m ⁻¹ |
| Curvature for Hill behavior c | -29.96 | -299.6 |
| Width for Hill behavior w | 0.45 | 0.4 |
| Optimal length l_{opt} | 0.9 m | 0.512 m |
| Angular coefficient for linear behavior μ | 0.25 | 0.25 |
| Maximum velocity v_{\max} | -3.5 m s ⁻¹ | -15 m s ⁻¹ |
| Curvature constant K | 1.5 | 5 |
| Dimensionless force constant | 1.5 | 1.5 |
| Damping coefficient d | 0.7 | 3450 |
| Segment length l_s | 1 m | 0.5773 m |
| Resting knee angle β | | 120° |
| Lever arm | | 0.04 m |

where a muscle in the upper link forces the leg to extend when activated. While the muscle from the previous model expanded when activated, this model contracts the muscle with activation. The equation of motion for this model follows the same behavior described at equation (1) without the damping contribution, as the output of the muscle will consider intrinsic damping properties that were embedded to simulate losses during hopping. The leg force is

$$F_{\text{leg}} = A(t) F_l F_v F_{\max} + d v_{\text{muscle}}, \quad (5)$$

where v_{muscle} is the muscle contraction speed, which is negative during takeoff and positive during landing, and d is the muscular damping coefficient. As it is expected, F_m will take into account F_{leg} combined with the mechanical advantage related to the geometry, as shown in

$$F_m = \frac{d_{\text{ma}}}{\sqrt{l_s^2 - (l_{\text{leg}}/2)^2}} F_{\text{leg}}, \quad (6)$$

with d_{ma} as the constant moment arm of the muscle, l_s the length of both upper and lower links, and l_{leg} as the distance between the body mass and the floor, as devised by [4]. The instantaneous length of the muscle can be calculated with

$$l_{\text{muscle}} = l_{\text{ref}} - d_{\text{ma}}(\beta - \beta_{\text{ref}}), \quad (7)$$

where l_{ref} is the reference length of the muscle, β is the joint angle and β_{ref} is the joint angle at which l_{ref} is reached.

Within our simulations the leg falls from an initial height with an initial resting length $l_0 = 1$, which is defined by

$$l_0 = 1.44 l_s \sqrt{1 - \cos(\beta_{\text{ref}})} = 1, \quad (8)$$

and alters the link length according to the resting knee angle. This results in a link length variation from

$l_s = 0.501$ to $l_s = 5.737$ with a proportional change in the maximum output force F_{\max} .

The definition for force–length and force–velocity relations for the two-segmented case differ in a few aspects from the linear model. Initially, the fact that the muscle contracts instead of expanding will likewise change force direction within both relations. Then, with the muscle and the damping element acting on the knee joint the everchanging angle will generate a nonlinear relationship between forces and leg length. Both relations are described as follows

$$F_l = \begin{cases} 1 & \text{Constant} \\ k(l - l_0) & \text{Linear} \\ \exp\left[-c \left| \frac{l - l_{\text{opt}}}{l_{\text{opt}} w} \right|^3\right] & \text{Hill} \end{cases} \quad (9)$$

$$F_v = \begin{cases} 1 & \text{Constant} \\ 1 + \mu v & \text{Linear} \\ \frac{v_{\max} - v}{v_{\max} + K v} & \text{Hill } (v > 0) \\ N + (N - 1) \frac{v_{\max} + v}{7.56 K v - v_{\max}} & \text{Hill } (v \leq 0), \end{cases} \quad (10)$$

where the meaning of each parameter is similar to the ones adopted at the linear model.

The parameters for this experiment are shown in table 1, and the rationale for these choices is to mimic observations with human experiments and simulations [4].

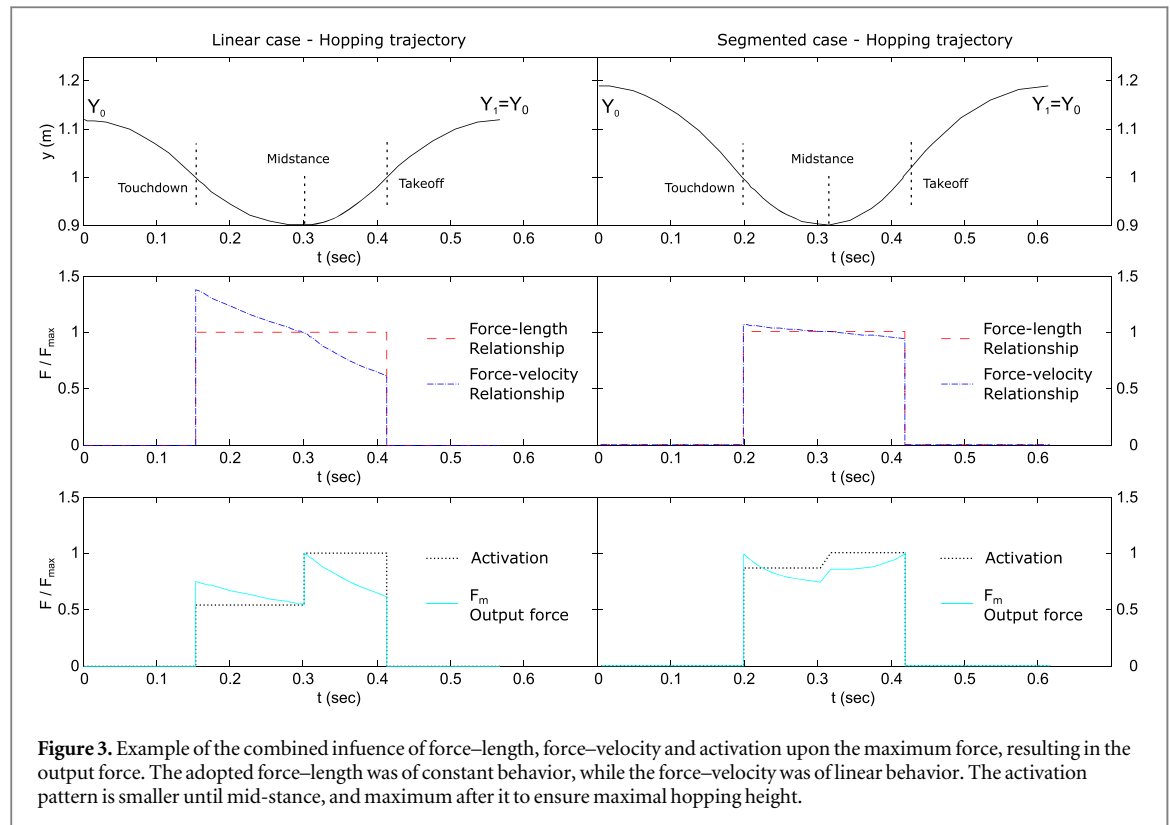
2.3. Muscle properties and activation

As demonstrated with equations (2), (5) and (6) the total force output from the model against the floor depends on the interplay between activation, force–length, force–velocity and maximum force. While figure 2 depicted the force–length and force–velocity relations, in figure 3 these parameters are combined with the activation and the maximum force to produce the output force.

The activation of our model is divided in two parts: before and after mid-stance. Initially, the activation has to enforce a maximal deformation of 0.1 m, where the mid-stance takes place. For this purpose, the simulation chooses one constant value for $A(t)$ until the deformation condition is met. Upon reaching mid-stance $A(t)$ is set to 1, the maximum value, and is kept in this setting until takeoff. Works such as [8] used a genetic algorithm to find an optimum activation pattern to fit the hopping period within 500 ms, and we decided to adopt a different method to 1. simplify the parameters during hopping and to 2. provide a new perspective and comparison between previous works and our contribution.

2.4. Hopping height and CoH

Our simulations sought to compare hopping heights for different force–length–velocity relations and, later,



perform similar comparison with their CoH. An inter-model comparison was not the focus of this work, as linear muscles have very low energy requirements and thus such comparison would be unfair. An intra-model comparison, though, can be strong enough to show trends from intrinsic properties when it comes to performance or efficiency.

A stable hopping height was chosen by iteratively starting simulations from hopping height y_0 and registering their final hopping height y_1 , and then adopting $y_0' = y_1$ as the new initial condition until the initial and final hopping height are equivalent ($y_0 = y_1$).

In previous works [13, 17] the idea of a CoH is proposed, as opposed to a cost of transport (CoT). While CoT focuses on horizontal energy expenditure, and grades robots and simulations by their planar displacement per consumed energy, the CoH compares the total energy input during hopping to the maximum potential energy (height) achieved. The formula used for such is

$$\text{CoH} = \frac{E_d}{mgy_1}, \quad (11)$$

where E_d is the energy loss due to damping. The addition of damping to the system allowed the system to lose energy during landing and takeoff, and if this loss was neglected, the total work of the system would have been conserved. As the damping dissipates energy, the muscle has to input energy to achieve the same height as the initial height. This energy input has a nonlinear nature, as it depends on complex force–length and force–velocity relations, but can be easily extrapolated when we consider that initial and final

height will incur in the same potential energy, as follows:

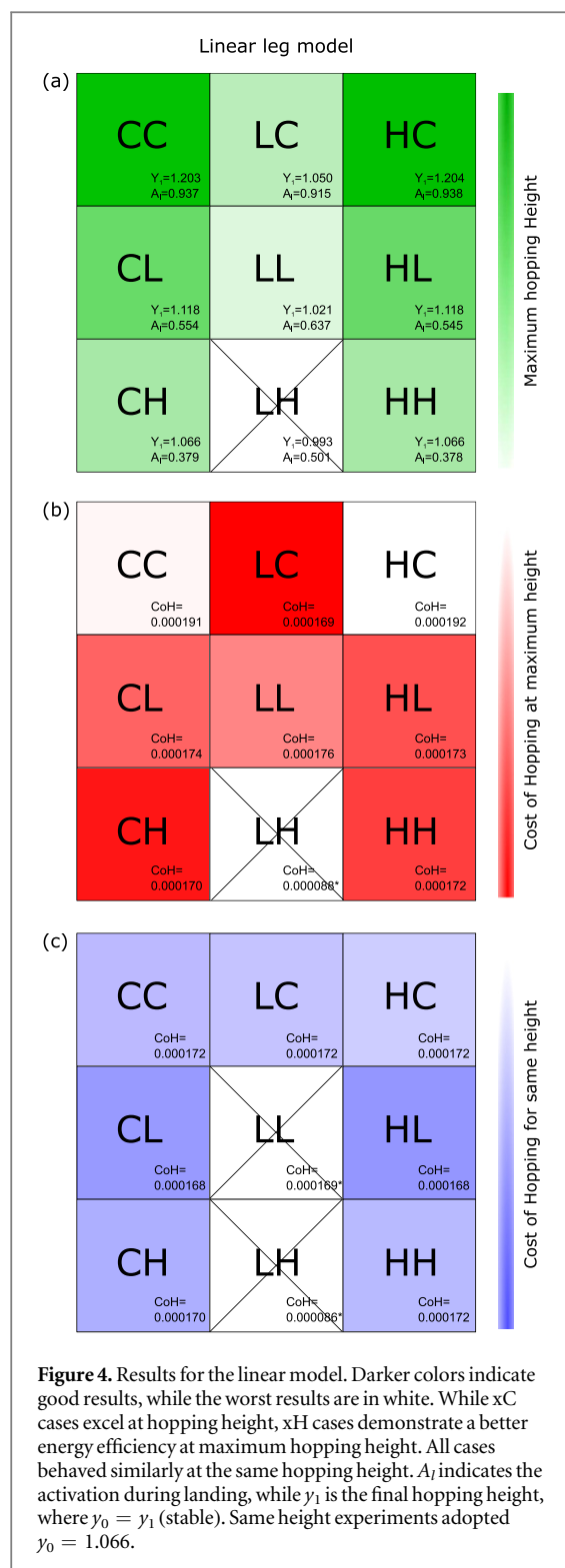
$$E_p(\text{initial}) = E_p(\text{final}) + E_{\text{input}} - E_d \rightarrow E_{\text{input}} - E_d = 0 \quad (12)$$

and the implications of damping as the sole source of energy loss are discussed at *study limitations*.

It is important to note that the damping coefficient d was artificially chosen for these experiments, and arbitrarily changing this parameter will result in different energy costs. In this vein, a comparison with biological data may be skewed by the choice of this parameter combined with total mass, leg length and other properties of the muscle. Moreover, as the damping element for the segmented case is acting upon the knee joint, a comparison between the results for linear and segmented models is not possible. For the sake of brevity, the cases will be called by an acronym with the combination of the first letters of each relation (e.g. constant force–length and Hill-type force–velocity will be called CH).

3. Results

Our initial experiments with the linear model aimed to create the groundwork for a comparison between this work and previous works from the field [8]. While adopting similar parameters, we added a damping force and a simplified activation pattern. As a result, a few differences between both results can be observed in the upper part of figure 4. The results show that the cases CC and HC obtained the highest hopping height,



with 1.203 m and 1.204 m, respectively. the cases CL and HL tied as the third best case, and the case LH could not reach a stable hopping condition.

Analyzing the energy lost due to damping within our linear experiments (figure 4(b)), the lowest CoH was found with the case LC, followed by CH and HH. With the exception of CC, HC and LH, all cases had similar CoH and there was a correlation between hopping height and CoH. A correlation between the activation pattern during landing, depicted as A_l , and the

CoH was not possible, as the lowest CoH (LC) demonstrated one of the highest A_l (0.915). Nonetheless, cases with a constant force–velocity relation (xC) demonstrated the best hopping height, while cases with a Hill-type force–velocity relation (xH) showed the best energy expenditure. A second linear experiment (figure 4(c)) considered the same hopping height observed at the HH case for all the proposed cases, and a high similarity of results is easily observed for all successful cases, with CoH values between 0.000168 and 0.000172. Although the LL and LH cases couldn't normally reach this hopping height, the LC case could when adopting a take-off activation pattern of $A = 1.1$.

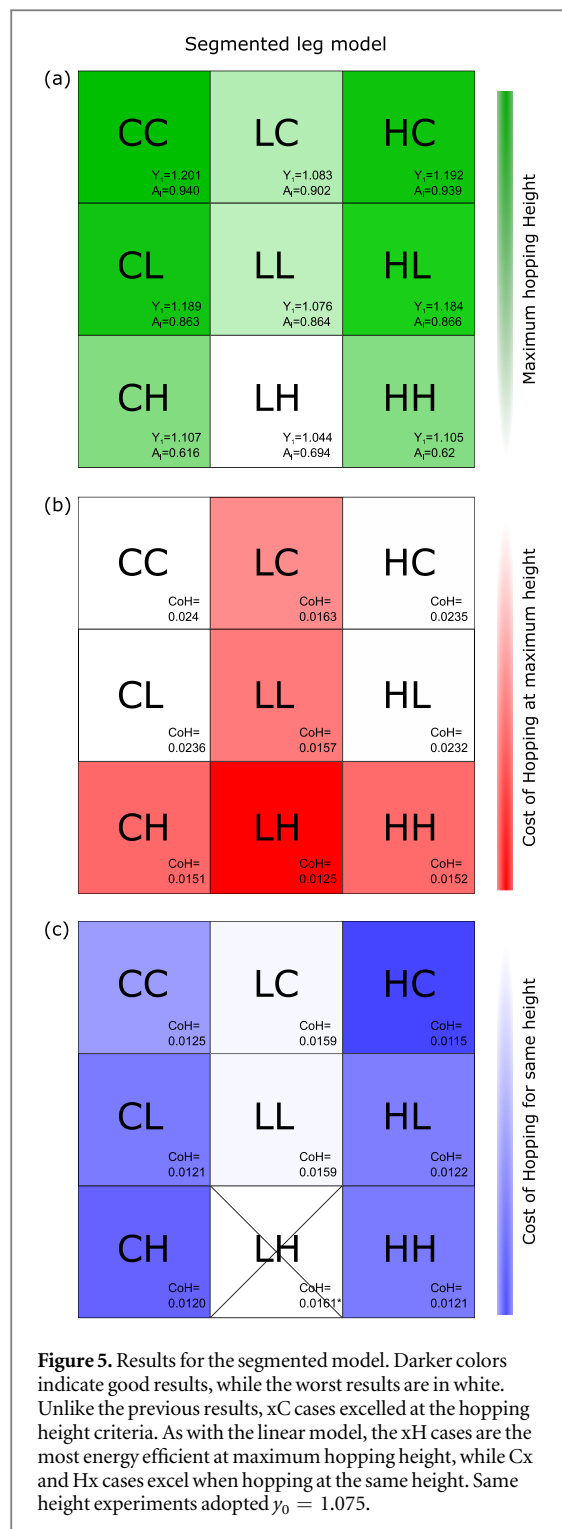
Experiments with the segmented model revealed that the introduction of a joint on the model drastically altered the outcome of our simulations. As seen in figure 5, the highest hopping height was observed on the constant force–velocity relations (xC), with the cases CC and HC demonstrating the highest stable hops. The presence of a higher A_l did not necessarily lead to a higher hopping height or a worse CoH.

The CoH for the segmented model followed a similar trend to the linear model, where the Hill-type force–velocity cases (xH) had superior energy efficiency. The lowest CoH during maximum hopping was found with the LH case, closely followed by the CH and HH case. While hopping at the same hopping height, the Hx cases demonstrated the best CoH, followed by the Cx cases, and the Lx cases were the least energy efficient.

The polarization of results among constant and Hill-type force–length–velocity relations prompted a fine-grained analysis of the cases CC, CH, HC and HH. Would the results be a consequence of the adopted resting knee angle $\beta = 120^\circ$? We probe the problem by hopping at maximum hopping height with different values for β , as shown in figure 6. These new experiments utilize a range of hopping angles from $\beta = 10^\circ$ to $\beta = 170^\circ$, and all cases adopted $l_0 = 1$. This condition results in legs in varying lengths (from 1.02 to 11.4m) and, consequently, the force output for each case varied accordingly (from 8.15 kN to 350.5 kN). These parameters were equally adopted for all four cases.

The cases xC and xH are starkly different when energy efficiency is considered, as the Hill-type force–velocity relation produces less energy losses at maximum hopping height. As the leg geometry straightens and the leg approaches the morphology of a human hopper, the overall energy efficiency worsens and the contributions from the force–length relations are felt. At angles $\beta > 90^\circ$, Cx cases became remarkably less energy efficient than Hx cases.

We decided to further study the behavior during landing and takeoff of the same four cases at $\beta = 150^\circ$, analyzing the velocity, damping force and power output during the stance phase, and the results are shown in figure 7. Both force output and power output



calculations are based on the damping losses. As the touchdown and liftoff speeds have the same absolute values, the total work during stance is zero. The damping energy loss, on the other hand, presents a force that is always opposite to the speed direction and produces a non-zero value, which represents the amount of energy lost by the muscle during stance.

The resemblances between CC and HC, and also between HH and CH, are clear. An explanation for the superior energy efficiency of the case HH over CH consists in the fact that HH had a shorter stance phase

with approximately the same damping force. The xC cases presented a remarkably high CoH, and figure 7 leads us to believe that, although shorter in duration, the xC cases always require a higher instantaneous power than the xH cases, which leads to higher amounts of energy loss per time.

A more in-depth analysis of these maximum hopping results shows that the energy efficiency during landing is worse for the HH case than the CH case (0.3 J), while the HH case has a better energy efficiency during takeoff (1.32 J), as seen in figure 8. Overall, the HH case outperforms the CH case for straight leg morphologies, as previously shown in figure 6.

4. Discussion

4.1. One-dimensional and two-segmented models

In this paper energy efficiency is inversely correlated to the amount of energy lost during hopping, and in this aspect the linear model is superior to the segmented model (figures 4 and 5), and the main explanation lies in the need for the segmented model to actuate the joints using a small moment arm, and thus requiring a greater output force. Many reasons led nature to develop such design, as segmented legs present a morphological advantage over telescopic legs in joint lubrication aspects or when obstacle clearance is required, as discussed by [18].

Previous simulations from [8] showed that, among linear models, the case CC obtained the best hopping height, and our results partially agree with their claim, as our best linear hopper adopted the HC case (as seen in figure 4). We argue that Hill-type force-length relations take more time to build up speed during takeoff, and, shall the previous work [8] unfreeze the hopping frequency condition (2 Hz), similar results will be obtained. Different activation patterns play a small role on the observed differences, since all simulations considered a full activation after mid-stance. Our findings with the segmented model, though, reinforce their claim, and the CC case obtained the highest hopping height, as shown in figure 5.

The nonlinearity introduced by the segmented model was better associated with *constant force-length relations* to reach higher hopping heights (figure 5), and this is in agreement with the results from the linear model (figure 4), consequently agreeing with the findings from [8].

When sheer performance is the objective, higher hopping heights can be obtained with a constant force-length-velocity relation with both models, although this kind of relation is not possible with biological actuators. Both models converged for the energy efficiency criteria at maximum hopping height, as the Hill-type force-velocity relation demonstrated the best CoH for both, and this demonstrates the higher energy efficiency present in animals during locomotion.

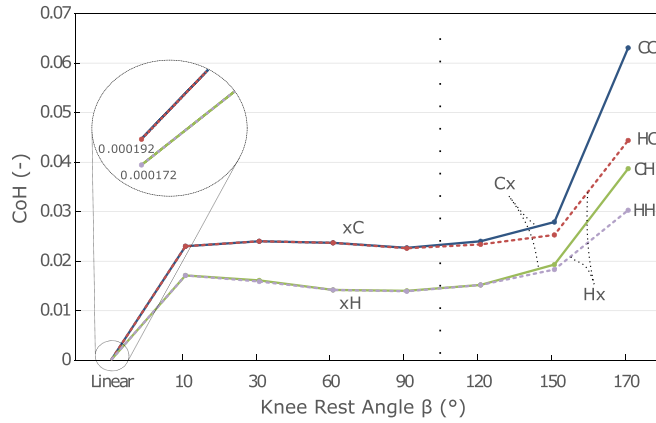


Figure 6. Different values for β result in different energy efficiencies for the cases xC and xH. As the knee resting angle increases ($\beta > 90^\circ$) the differences between Cx and Hx can also be seen. The condition $l_0 = 1$ was kept for all experiments, and the link geometries obeyed the equation (8).

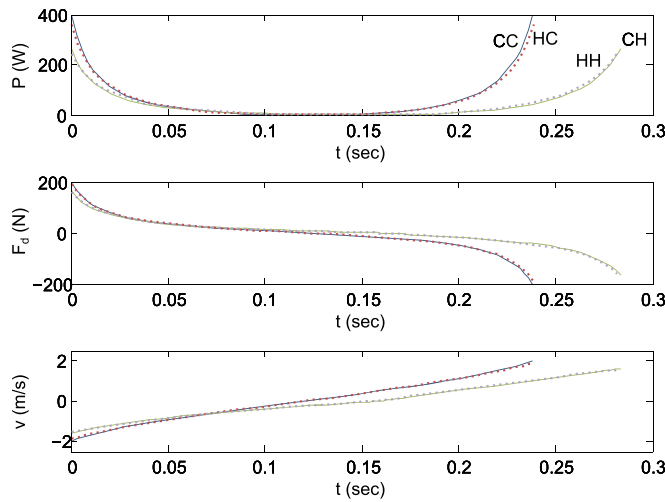


Figure 7. Comparison among the four cases. It is clear that the cases CC and HC require more power for a shorter period, while the cases HH and CH waste less power for longer periods. HH uses approximately the same amount of power that CH uses, but for a shorter period during maximum hopping.

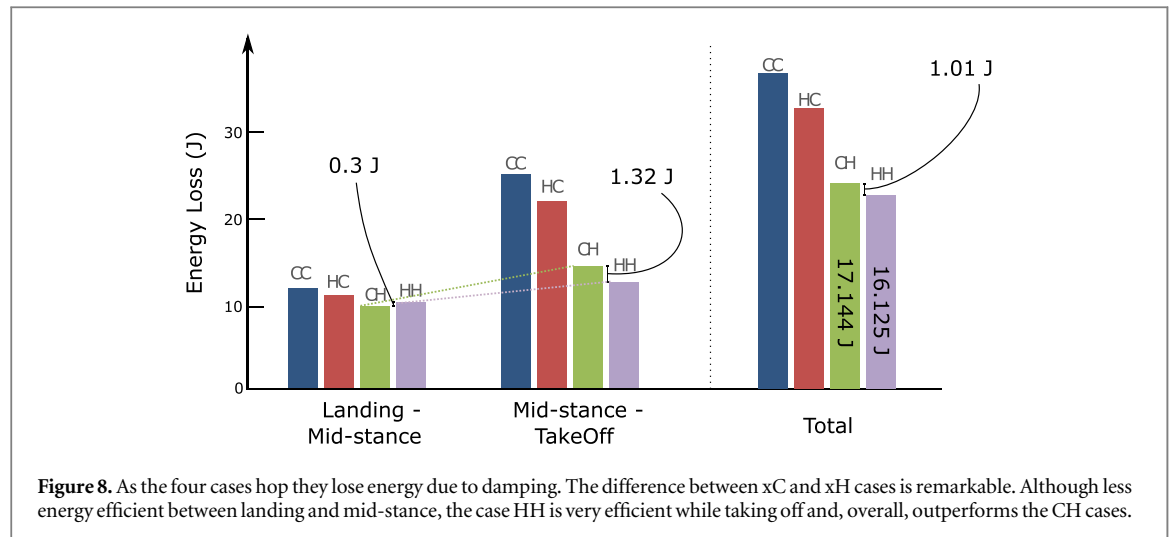
4.2. Influence of resting angle on energy efficiency

In [18], it is stated that human-like segmented legs are superior to other designs when energy efficiency and stability are considered. Our simulations with different knee angles showed that for angles above 90° , which are straighter and closer to the human landing angle, the Hill-type force–length–velocity was the most energy efficient, and this strongly agrees with the previous hypothesis from [18]. A clear explanation for this phenomenon is that different landing angles require different leg lengths, which incur in different muscular velocities. Although a low variability was observed between 10° and 170° , our future works will explore different leg geometries to explore other possible outcomes.

As the highest energy efficiency (low CoH) was found with leg geometries between 60° and 90° , we can infer that differences between HH and CH would not be

significant with these geometries (as seen in the colinearity of xH cases in figure 6), and the Hill-type force–velocity relation would be the most important trait leading to a higher energy efficiency. *This connotes that roboticists can reap the benefits of segmented legs by designing their robots with landing angles between these values, and preferably adopt actuators capable of replicating a biomimetic force–velocity relation, such as [19].* Previous works [4, 8] did not approach the energy efficiency problem nor its interplay with knee angles, and the contribution of this work is unique in these aspects.

Our simulations focused on the linear and the segmented models, and our next research steps will focus on different morphologies to fully test the hypothesis from [18] pertaining the optimality of the human segmented morphology and further extend contributions on locomotory efficiency.



4.3. Hopping height and CoH trade-off

A very clear trend is visible while analyzing the hopping height for all 18 cases: within every column, the maximum hopping height decreased from xC to xL, and kept this same trend from xL to xH. The same kind of relationship is present within the CoH columns, and it leads us to state that a correlation between these two does exist. The proportionality of the relationship, however, is not clearly seen among hops with the same height, and figures 4(c) and 5(c) depict an interplay between constant and Hill-type relations leading to higher efficiencies. Further, linear force–length relations presented itself as the worst alternative for both hopping height and CoH at the same height and for both models. These results should prompt roboticists to consider which actuation method to avoid, as combustion engines and electrical motors have different relationships between their rotational speed and torque, which could be decisive to determine the energy efficiency and hopping height within a physical experiment, such as [20].

A similar analysis between hopping height, energy efficiency and force–length–velocity relations is not present in previous works, but in [8] a correlation between force–velocity and stability is made. Within our simulations for both models, the cases CH and HH demonstrated a remarkable energy efficiency combined with an average hopping height. These findings, combined with the stability association made by [8], allow us to infer that *Hill-type force–velocity relations increase stability while decreasing energy consumption*. The generalization for the stability claims from the linear model to the segmented model still remains to be investigated.

In strong agreement with the results from [8], the simplest muscle models obtained the highest hopping heights, but ironically they were also the ones with the worst energy efficiency. All the xC cases required an activation superior to 0.9 for both linear and segmented models, while all the xH cases demonstrated an $A_l < 0.7$. As explained in [8], ‘in the more complex

models the factors in the force equation of the muscle model mostly reduce the maximum dynamic muscle force’, and thus lower hopping heights should be expected in xH cases.

4.4. Study limitations and conclusions

As in any experiment in which biological conditions are recreated artificially, our study is limited by the degree of simplification from our system. While musculoskeletal systems are capable of providing more realistic hopping behavior results, the main benefit of a simpler simulation is that un-necessary parameters, noise and disturbances are eliminated, and our results can concentrate on the phenomenon under observation. A few research settings show potential to approach this similar subject with real-world experiments, and this limitation can be addressed properly [20]. Damping losses through the parallel damper were considered as the only source of losses on this simulation, and therefore the energy input from the muscles was the precise amount needed to replenish this loss. In real life experiments many other sources of energy loss exist, and future works in this area should account for additional contributions.

In this work we analyzed 18 different hopping conditions, combined force–length and force–velocity relations to two different hopping models, and we found that the results differ between linear and segmented models. The nonlinearity introduced by the segmented model did not affect the conclusions from [8], as the constant force–velocity relations also reached higher hopping height for both models. Both models converged for the energy efficiency criteria at maximum hopping height, as the Hill-type force–velocity relation demonstrated the best results for both. This superiority is not obvious when hopping at the same height, as the HC emerged as the best option for segmented legs, followed by CH and HH. Segmented models with a hopping angle between 60° and 90° reached the best energy efficiency, and, independently of the adopted force–length–velocity ratio, this value

should be used as a standard for robots with segmented legs.

In the future we will perform new simulations with a higher complexity level by introducing stretch-reflex responses, segment differences, and a third link, and we will assess the contribution from these degrees of complexity to the overall hopping efficiency.

Acknowledgments

This research was supported by the RoboSoft—Coordination Action for Soft Robotics, funded by the European Commission under the Future and Emerging Technologies—(FP7-ICT-2013-C project no 619319).

References

- [1] Daley M 2008 Biomechanics: running over uneven terrain is a no-brainer *Curr. Biol.* **18** 1064–6
- [2] Melvil Jones G and Watt D G D 1971 Observations on the control of stepping and hopping movements in man *J. Physiol.* **219** 709–27
- [3] Dyhre-Poulsen P, Simonsen E B and Voigt M 1991 Dynamic control of muscle stiffness and H reflex modulation during hopping and jumping in man *J. Physiol.* **437** 287–304
- [4] Geyer H, Seyfarth A and Blickhan R 2003 Positive force feedback in bouncing gaits *Proc. R. Soc. London B* **270** 2173–83
- [5] Lepora N F, Verschure P and Prescott T J 2013 The state of the art in biomimetics *Bioinspir. Biomim.* **8** 013001
- [6] Rosendo A, Liu X, Shimizu M and Hosoda K 2015 Stretch reflex improves rolling stability during hopping of a decerebrate biped system *Bioinspir. Biomim.* **10** 016008
- [7] Haeufle D F B, Grimmer S, Kalveram K T and Seyfarth A 2012 Integration of intrinsic muscle properties, feed-forward and feedback signals for generating and stabilizing hopping *J. R. Soc. Interface* **9** 1458–69
- [8] Haeufle D F B, Grimmer S and Seyfarth A 2010 The role of intrinsic muscle properties for stable hopping—stability is achieved by the force–velocity relation *Bioinspir. Biomim.* **5** 016004
- [9] Sockol M D, Raichlen D A and Pontzer H 2007 Chimpanzee locomotor energetics and the origin of human bipedalism *Proc. Natl Acad. Sci.* **104** 12265–9
- [10] Tucker V A 1975 The energetic cost of moving about: walking and running are extremely inefficient forms of locomotion. Much greater efficiency is achieved by birds, fish—and bicyclists *Am. Sci.* **63** 413–9
- [11] McGeer T 1990 Passive dynamic walking *Int. J. Robot. Res.* **9** 62–82
- [12] Ananthanarayanan A, Azadi M and Kim S 2012 Towards a bio-inspired leg design for high-speed running *Bioinspir. Biomim.* **7** 046005
- [13] Yu X and Iida F 2014 Minimalistic models of an energy-efficient vertical-hopping robot *IEEE Trans. Mechatronics* **61** 1053–62
- [14] Gunther F, Giardina F and Iida F 2014 Self-stable one-legged hopping using a curved foot *IEEE Int. Conf. Robotics and Automation* pp 5133–8
- [15] Sharbafi M A, Maufroy C, Ahmadabadi M N, Yazdanpanah M J and Seyfarth A 2013 Robust hopping based on virtual pendulum posture control *Bioinspir. Biomim.* **8** 036002
- [16] Rosendo A, Narioka K and Hosoda K 2012 Muscles roles on directional change during hopping of a biomimetic feline hindlimb *Proc. IEEE Int. Conf. Robotics and Biomim. ROBIO, Guangzhou (China, 11–14 December 2012)* (Piscataway, NJ: IEEE) (doi:10.1109/ROBIO.2012.6491108)
- [17] Grabowski A M and Herr H M 2009 Leg exoskeleton reduces the metabolic cost of human hopping *J. Appl. Physiol.* **107** 670–8
- [18] Blickhan R, Seyfarth A, Geyer H, Grimmer S, Wagner H and Gunther M 2006 Intelligence by mechanics *Phil. Trans. R. Soc. A* **365** 199–220
- [19] Azizi E and Roberts T J 2013 Variable gearing in a biologically inspired pneumatic actuator array *Bioinspir. Biomim.* **8** 026002
- [20] Seyfarth A, Kalveram K T and Geyer H 2007 Simulating muscle-reflex dynamics in a simple hopping robot *Proc. of Fachgespräche Autonome Mobile Systeme* (Springer) p 294300